Available online at www.sciencedirect.com
SCIENCE DIRECT®
Polymer 45 (2004) 321–335
polymer
www.elsevier.com/locate/polymer

Molecular weight distributions in styrene polymerization with asymmetric bifunctional initiators

M. Asteasuain, A. Brandolin*, C. Sarmoria

Planta Piloto de Ingeniería Química - UNS-CONICET, Camino La Carrindanga, km 7, 8000 Bahía Blanca, Argentina

Received 5 September 2003; received in revised form 23 October 2003; accepted 30 October 2003

Abstract

We model the molecular weight distribution (MWD) of polystyrene obtained using asymmetric bifunctional initiators. We do that by extending an existing model able to predict conversions and average molecular weights. By applying probability generating functions to the mass balances, a finite set of differential equations is obtained. This set must be solved and numerically inverted in order to obtain the MWD. Validation was performed using available experimental data on average molecular weights. Those calculated from the predicted MWD agree well with the reported experimental data. In order to show the potential of the model as a tool to tailor MWD, we use it to evaluate operating conditions in a batch reactor that would result in bimodal MWD.

Keywords: Polystyrene; Bifunctional initiators; MWD

1. Introduction

It has been shown both experimentally and theoretically that the use of asymmetric bifunctional initiators for free-radical polymerization presents several advantages [1–5]. It allows synthesis of high molecular weight polymer at high temperatures, leading to short reaction cycles with the ensuing economic advantage. Furthermore, the molecular weights obtained are significantly higher than those achieved either with monofunctional initiators or mixtures of monofunctional initiators at equivalent initial concentrations.

From the modeling point of view, the bulk polymerization of styrene with this kind of initiator presents several challenges. At high conversions the viscosity increase causes the reaction to become diffusion-controlled. The two reactive moieties in the initiator, even if they have very different decomposition kinetic rate constants, are simultaneously active. Initiation and reinitiation of chains also needs to be considered.

In the work of Kim and Choi [1] a mathematical model for the free-radical polymerization of styrene with asymmetric initiator is presented that takes diffusion control at high conversions into account. The model allows calculation of average molecular chain lengths, conversions, and the concentration of lumped species such as dead polymer, polymer with one undecomposed peroxide group or radicals with two active sites, among others. The complete molecular weight distribution (MWD) may not be calculated using their model. Other authors [2–5] undertook similar efforts, where again several quantities could be calculated but not the complete MWD. The approximate model of O'Driscoll and Bevington [6] could simulate the MWD under rather severe assumptions; it gave insight into the process but could not tackle real-world occurrences such as gel effect. Since MWD affects the end-use properties of the synthesized polymer, it is of interest to be able to predict it for conditions closely resembling those in the actual polymerization.

In this work we present a mathematical model based on the probability generating function (pgf) transform [7–8] that allows prediction of the complete MWD. We use the same kinetic mechanism proposed by Kim and Choi [1] and Kim [9]. Our predictions coincide with theirs in those quantities that could be calculated with their model, but in addition we are successful at predicting complete MWD.

* Corresponding author. Tel.: +54-914861700x272; fax: +54-914861600.
E-mail addresses: abrandolin@plapiqui.edu.ar (A. Brandolin), masteasuain@plapiqui.edu.ar (M. Asteasuain), csarmoria@plapiqui.edu.ar (C. Sarmoria).

0032-3861/$ - see front matter © 2003 Elsevier Ltd. All rights reserved.
doi:10.1016/j.polymer.2003.10.083

The averages of the predicted MWD agree well with experimentally measured quantities, obtained for the polymerization of styrene with 4-(t-butyl peroxy carbonyl-3-hexyl-6-[7 -(t-butyl peroxy carbonyl) heptyl] cyclo hexene as initiator [9]. The model is able to predict changes in MWD due to operating temperature and initial initiator concentration. We also show that it is possible to tailor the MWD through changes in the operating conditions, making even bimodal distributions in polystyrene possible.

2. Mathematical model

In this model we make use of the kinetic steps proposed by Kim and Choi [1] and Kim [9], which are shown below (Eqs. (1)–(35))

Peroxide decomposition

In initiators

$$\mathrm{I} \xrightarrow{k_{d_B}} \mathrm{R}^{\cdot} + \mathrm{R}^{\cdot \mathrm{A}} \tag{1}$$

$$\mathrm{I} \xrightarrow{k_{d_A}} \mathrm{R}^{\cdot} + \mathrm{R}^{\cdot \mathrm{B}} \tag{2}$$

In initiation radicals

$$\mathrm{R}^{\cdot \mathrm{A}} \xrightarrow{k_{d_A}} \mathrm{R}^{\cdot} + \mathrm{R}^{\cdot\cdot} \tag{3}$$

$$\mathrm{R}^{\cdot \mathrm{B}} \xrightarrow{k_{d_B}} \mathrm{R}^{\cdot} + \mathrm{R}^{\cdot\cdot} \tag{4}$$

In macroradicals

$$\mathrm{R}_n^{\cdot \mathrm{A}} \xrightarrow{k_{d_A}} \mathrm{R}^{\cdot} + \mathrm{R}_n^{\cdot\cdot} \qquad n = 1, \ldots, \infty \tag{5}$$

$$\mathrm{R}_n^{\cdot \mathrm{B}} \xrightarrow{k_{d_B}} \mathrm{R}^{\cdot} + \mathrm{R}_n^{\cdot\cdot} \qquad n = 1, \ldots, \infty \tag{6}$$

In temporary polymers

$$\mathrm{P}_n^{\mathrm{A}} \xrightarrow{k_{d_A}} \mathrm{R}^{\cdot} + \mathrm{R}_n^{\cdot} \qquad n = 1, \ldots, \infty \tag{7}$$

$$\mathrm{P}_n^{\mathrm{B}} \xrightarrow{k_{d_B}} \mathrm{R}^{\cdot} + \mathrm{R}_n^{\cdot} \qquad n = 1, \ldots, \infty \tag{8}$$

$$\mathrm{P}_n^{\mathrm{AB}} \xrightarrow{k_{d_A}} \mathrm{R}^{\cdot} + \mathrm{R}_n^{\cdot \mathrm{B}} \qquad n = 2, \ldots, \infty \tag{9}$$

$$\mathrm{P}_n^{\mathrm{AB}} \xrightarrow{k_{d_B}} \mathrm{R}^{\cdot} + \mathrm{R}_n^{\cdot \mathrm{A}} \qquad n = 2, \ldots, \infty \tag{10}$$

$$\mathrm{P}_n^{\mathrm{AA}} \xrightarrow{2k_{d_A}} \mathrm{R}^{\cdot} + \mathrm{R}_n^{\cdot \mathrm{A}} \qquad n = 2, \ldots, \infty \tag{11}$$

$$\mathrm{P}_n^{\mathrm{BB}} \xrightarrow{2k_{d_B}} \mathrm{R}^{\cdot} + \mathrm{R}_n^{\cdot \mathrm{B}} \qquad n = 2, \ldots, \infty \tag{12}$$

Initiation

$$\mathrm{R}^{\cdot} + \mathrm{M} \xrightarrow{k_i} \mathrm{R}_1^{\cdot} \tag{13}$$

$$\mathrm{R}^{\cdot \mathrm{A}} + \mathrm{M} \xrightarrow{k_i} \mathrm{R}_1^{\cdot \mathrm{A}} \tag{14}$$

$$\mathrm{R}^{\cdot \mathrm{B}} + \mathrm{M} \xrightarrow{k_i} \mathrm{R}_1^{\cdot \mathrm{B}} \tag{15}$$

$$\mathrm{R}^{\cdot\cdot} + \mathrm{M} \xrightarrow{2k_i} \mathrm{R}_1^{\cdot\cdot} \tag{16}$$

$$3\mathrm{M} \xrightarrow{k_{dm}} 2\mathrm{R}_1^{\cdot} + \mathrm{M}' \ (\textit{Thermal Initiation}) \tag{17}$$

Propagation

$$\mathrm{R}_n^{\cdot} + \mathrm{M} \xrightarrow{k_p} \mathrm{R}_{n+1}^{\cdot} \qquad n = 1, \ldots, \infty \tag{18}$$

$$\mathrm{R}_n^{\cdot \mathrm{A}} + \mathrm{M} \xrightarrow{k_p} \mathrm{R}_{n+1}^{\cdot \mathrm{A}} \qquad n = 1, \ldots, \infty \tag{19}$$

$$\mathrm{R}_n^{\cdot \mathrm{B}} + \mathrm{M} \xrightarrow{k_p} \mathrm{R}_{n+1}^{\cdot \mathrm{B}} \qquad n = 1, \ldots, \infty \tag{20}$$

$$\mathrm{R}_n^{\cdot\cdot} + \mathrm{M} \xrightarrow{2k_p} \mathrm{R}_{n+1}^{\cdot\cdot} \qquad n = 1, \ldots, \infty \tag{21}$$

Chain transfer to monomer

$$\mathrm{R}_n^{\cdot} + \mathrm{M} \xrightarrow{k_{fm}} \mathrm{P}_n + \mathrm{R}_1^{\cdot} \qquad n = 1, \ldots, \infty \tag{22}$$

$$\mathrm{R}_n^{\cdot \mathrm{A}} + \mathrm{M} \xrightarrow{k_{fm}} \mathrm{P}_n^{\mathrm{A}} + \mathrm{R}_1^{\cdot} \qquad n = 1, \ldots, \infty \tag{23}$$

$$\mathrm{R}_n^{\cdot \mathrm{B}} + \mathrm{M} \xrightarrow{k_{fm}} \mathrm{P}_n^{\mathrm{B}} + \mathrm{R}_1^{\cdot} \qquad n = 1, \ldots, \infty \tag{24}$$

$$\mathrm{R}_n^{\cdot\cdot} + \mathrm{M} \xrightarrow{2k_{fm}} \mathrm{R}_n^{\cdot} + \mathrm{R}_1^{\cdot} \qquad n = 1, \ldots, \infty \tag{25}$$

Termination by combination

$$\mathrm{R}_n^{\cdot} + \mathrm{R}_m^{\cdot} \xrightarrow{k_t} \mathrm{P}_{n+m} \qquad n, m = 1, \ldots \infty \tag{26}$$

$$\mathrm{R}_n^{\cdot} + \mathrm{R}_m^{\cdot \mathrm{A}} \xrightarrow{k_t} \mathrm{P}_{n+m}^{\mathrm{A}} \qquad n, m = 1, \ldots \infty \tag{27}$$

$$\mathrm{R}_n^{\cdot} + \mathrm{R}_m^{\cdot \mathrm{B}} \xrightarrow{k_t} \mathrm{P}_{n+m}^{\mathrm{B}} \qquad n, m = 1, \ldots \infty \tag{28}$$

$$\mathrm{R}_n^{\cdot} + \mathrm{R}_m^{\cdot\cdot} \xrightarrow{2k_t} \mathrm{R}_{n+m}^{\cdot} \qquad n, m = 1, \ldots \infty \tag{29}$$

$$\mathrm{R}_n^{\cdot \mathrm{A}} + \mathrm{R}_m^{\cdot \mathrm{A}} \xrightarrow{k_t} \mathrm{P}_{n+m}^{\mathrm{AA}} \qquad n, m = 1, \ldots \infty \tag{30}$$

$$\mathrm{R}_n^{\cdot \mathrm{A}} + \mathrm{R}_m^{\cdot \mathrm{B}} \xrightarrow{k_t} \mathrm{P}_{n+m}^{\mathrm{AB}} \qquad n, m = 1, \ldots \infty \tag{31}$$

$$\mathrm{R}_n^{\cdot \mathrm{A}} + \mathrm{R}_m^{\cdot\cdot} \xrightarrow{2k_t} \mathrm{R}_{n+m}^{\cdot \mathrm{A}} \qquad n, m = 1, \ldots \infty \tag{32}$$

$$\mathrm{R}_n^{\cdot \mathrm{B}} + \mathrm{R}_m^{\cdot \mathrm{B}} \xrightarrow{k_t} \mathrm{P}_{n+m}^{\mathrm{BB}} \qquad n, m = 1, \ldots \infty \tag{33}$$

$$\mathrm{R}_n^{\cdot \mathrm{B}} + \mathrm{R}_m^{\cdot\cdot} \xrightarrow{2k_t} \mathrm{R}_{n+m}^{\cdot \mathrm{B}} \qquad n, m = 1, \ldots \infty \tag{34}$$

$$\mathrm{R}_n^{\cdot\cdot} + \mathrm{R}_m^{\cdot\cdot} \xrightarrow{4k_t} \mathrm{R}_{n+m}^{\cdot\cdot} \qquad n, m = 1, \ldots \infty \tag{35}$$

In these equations, I is the bifunctional peroxide initiator, $\mathrm{R}^{\cdot}$ is an initiation radical, $\mathrm{R}_n^{\cdot}$ a macroradical of chain length n and P_n a polymer of chain length n. The superscripts indicate the type of end unit/units that identify each molecule: $\cdot$ stands for a radical active center, A for an undecomposed A peroxide group, and B for an undecomposed B peroxide group. Notice that some species may present different combination of end units. For instance, $\mathrm{R}_n^{\cdot\cdot}$ is a macroradical with active centers in both chain ends, $\mathrm{P}_n^{\mathrm{AB}}$ is a polymer with undecomposed A and B peroxide groups, etc.

This kinetic mechanism leads to ten macromolecular species coexisting in the reacting mixture: macroradicals $\mathrm{R}_n^{\cdot}$, $\mathrm{R}_n^{\cdot \mathrm{A}}$, $\mathrm{R}_n^{\cdot \mathrm{B}}$ and $\mathrm{R}_n^{\cdot\cdot}$, temporary polymers $\mathrm{P}_n^{\mathrm{A}}$, $\mathrm{P}_n^{\mathrm{B}}$, $\mathrm{P}_n^{\mathrm{AB}}$, $\mathrm{P}_n^{\mathrm{AA}}$

and P_n^{BB}, and permanent polymer P_n. Mass balance equations must be derived for each of them, as well as for peroxide initiators, initiation radicals and monomer (Eqs. (36)–(51)).

Initiators

$$\frac{1}{V}\frac{d(IV)}{dt} = -(k_{d_A} + k_{d_B})I \tag{36}$$

Initiation radicals

$$\frac{1}{V}\frac{d(R^{\cdot A}V)}{dt} = fk_{d_B}I - k_{d_A}R^{\cdot A} - k_iR^{\cdot A}M \tag{37}$$

$$\frac{1}{V}\frac{d(R^{\cdot B}V)}{dt} = fk_{d_A}I - k_{d_B}R^{\cdot B} - k_iR^{\cdot B}M \tag{38}$$

$$\begin{aligned}\frac{1}{V}\frac{d(R^{\cdot}V)}{dt} = {} & f[(k_{d_A} + k_{d_B})I + k_{d_A}R^{\cdot A} + k_{d_B}R^{\cdot B} \\ & + k_{d_A}(Y_0^{\cdot A} + M_0^A + M_0^{AB} + 2M_0^{AA}) \\ & + k_{d_B}(Y_0^{\cdot B} + M_0^B + M_0^{AB} + 2M_0^{BB})] \\ & - k_iR^{\cdot}M\end{aligned} \tag{39}$$

$$\frac{1}{V}\frac{d(R^{\cdot\cdot}V)}{dt} = f(k_{d_A}R^{\cdot A} + k_{d_B}R^{\cdot B}) - 2k_iR^{\cdot\cdot}M \tag{40}$$

Monomer

$$\begin{aligned}\frac{1}{V}\frac{d(MV)}{dt} = {} & -3k_{dm}M^3 - k_i(R^{\cdot} + R^{\cdot A} + R^{\cdot B} + 2R^{\cdot\cdot})M \\ & - k_{fm}M(Y_0^{\cdot} + Y_0^{\cdot A} + Y_0^{\cdot B} + 2Y_0^{\cdot\cdot}) \\ & - k_pM(Y_0^{\cdot} + Y_0^{\cdot A} + Y_0^{\cdot B} + 2Y_0^{\cdot\cdot})\end{aligned} \tag{41}$$

Macroradicals

$$\begin{aligned}\frac{1}{V}\frac{d(R_n^{\cdot}V)}{dt} = {} & 2k_{dm}M^3\delta_{n,1} + k_iR^{\cdot}M\delta_{n,1} + k_{d_A}P_n^A \\ & + k_{d_B}P_n^B + k_pMR_{n-1}^{\cdot}(1-\delta_{n,1}) \\ & - k_pMR_n^{\cdot} + k_{fm}M(Y_0^{\cdot} + Y_0^{\cdot A} + Y_0^{\cdot B} + 2Y_0^{\cdot\cdot})\delta_{n,1} \\ & + k_{fm}M(2R_n^{\cdot\cdot} - R_n^{\cdot}) - k_tR_n^{\cdot}(Y_0^{\cdot} + Y_0^{\cdot A} + Y_0^{\cdot B} \\ & + 2Y_0^{\cdot\cdot}) + 2k_t\sum_{m=1}^{n-1}R_{n-m}^{\cdot}R_m^{\cdot\cdot}(1-\delta_{n,1}) \\ & n = 1,\ldots\infty\end{aligned} \tag{42}$$

$$\begin{aligned}\frac{1}{V}\frac{d(R_n^{\cdot A}V)}{dt} = {} & k_iR^{\cdot A}M\delta_{n,1} - k_{d_A}R_n^{\cdot A} + (k_{d_B}P_n^{AB} + 2k_{d_A}P_n^{AA}) \\ & (1-\delta_{n,1}) + k_pMR_{n-1}^{\cdot A}(1-\delta_{n,1}) - k_pMR_n^{\cdot A} \\ & - k_{fm}MR_n^{\cdot A} - k_tR_n^{\cdot A}(Y_0^{\cdot} + Y_0^{\cdot A} + Y_0^{\cdot B} + 2Y_0^{\cdot\cdot}) \\ & + 2k_t\sum_{m=1}^{n-1}R_{n-m}^{\cdot A}R_m^{\cdot\cdot}(1-\delta_{n,1}) \qquad n = 1,\ldots\infty\end{aligned} \tag{43}$$

$$\begin{aligned}\frac{1}{V}\frac{d(R_n^{\cdot B}V)}{dt} = {} & k_iR^{\cdot B}M\delta_{n,1} - k_{d_B}R_n^{\cdot B} + (k_{d_A}P_n^{AB} + 2k_{d_B}P_n^{BB}) \\ & (1-\delta_{n,1}) + k_pMR_{n-1}^{\cdot B}(1-\delta_{n,1}) - k_pMR_n^{\cdot B} \\ & - k_{fm}MR_n^{\cdot B} - k_tR_n^{\cdot B}(Y_0^{\cdot} + Y_0^{\cdot A} + Y_0^{\cdot B} + 2Y_0^{\cdot\cdot}) \\ & + 2k_t\sum_{m=1}^{n-1}R_{n-m}^{\cdot B}R_m^{\cdot\cdot}(1-\delta_{n,1}) \qquad n = 1,\ldots\infty\end{aligned} \tag{44}$$

$$\begin{aligned}\frac{1}{V}\frac{d(R_n^{\cdot\cdot}V)}{dt} = {} & 2k_iR^{\cdot\cdot}M\delta_{n,1} + k_{d_A}R_n^{\cdot A} + k_{d_B}R_n^{\cdot B} \\ & + 2k_pMR_{n-1}^{\cdot\cdot}(1-\delta_{n,1}) - 2k_pMR_n^{\cdot\cdot} - 2k_{fm}MR_n^{\cdot\cdot} \\ & - 2k_tR_n^{\cdot\cdot}(Y_0^{\cdot} + Y_0^{\cdot A} + Y_0^{\cdot B} + 2Y_0^{\cdot\cdot}) \\ & + 2k_t\sum_{m=1}^{n-1}R_{n-m}^{\cdot\cdot}R_m^{\cdot\cdot}(1-\delta_{n,1}) \qquad n = 1,\ldots\infty\end{aligned} \tag{45}$$

Temporary polymers

$$\begin{aligned}\frac{1}{V}\frac{d(P_n^AV)}{dt} = {} & -k_{d_A}P_n^A + k_{fm}MR_n^{\cdot A} \\ & + k_t\sum_{m=1}^{n-1}R_{n-m}^{\cdot}R_m^{\cdot A}(1-\delta_{n,1}) \qquad n = 1,\ldots\infty\end{aligned} \tag{46}$$

$$\begin{aligned}\frac{1}{V}\frac{d(P_n^BV)}{dt} = {} & -k_{d_B}P_n^B + k_{fm}MR_n^{\cdot B} \\ & + k_t\sum_{m=1}^{n-1}R_{n-m}^{\cdot}R_m^{\cdot B}(1-\delta_{n,1}) \qquad n = 1,\ldots\infty\end{aligned} \tag{47}$$

$$\begin{aligned}\frac{1}{V}\frac{d(P_n^{AB}V)}{dt} = {} & \left(-(k_{d_A} + k_{d_B})P_n^{AB} + k_t\sum_{m=1}^{n-1}R_{n-m}^{\cdot A}R_m^{\cdot B}\right) \\ & (1-\delta_{n,1}) \qquad n = 1,\ldots\infty\end{aligned} \tag{48}$$

$$\begin{aligned}\frac{1}{V}\frac{d(P_n^{AA}V)}{dt} = {} & \left(-2k_{d_A}P_n^{AA} + \frac{1}{2}k_t\sum_{m=1}^{n-1}R_{n-m}^{\cdot A}R_m^{\cdot A}\right) \\ & (1-\delta_{n,1}) \qquad n = 1,\ldots\infty\end{aligned} \tag{49}$$

$$\frac{1}{V}\frac{\mathrm{d}(\mathrm{P}_n^{\mathrm{BB}}V)}{\mathrm{d}t} = \left(-2k_{\mathrm{d_B}}\mathrm{P}_n^{\mathrm{BB}} + \frac{1}{2}k_{\mathrm{t}}\sum_{m=1}^{n-1}\mathrm{R}_{n-m}^{\cdot\mathrm{B}}\mathrm{R}_m^{\cdot\mathrm{B}} \right) \qquad (50)$$

$$(1-\delta_{n,1}) \qquad n = 1,\ldots\infty$$

Permanent polymer

$$\frac{1}{V}\frac{\mathrm{d}(\mathrm{P}_n V)}{\mathrm{d}t} = k_{\mathrm{fm}}M\mathrm{R}_n^{\cdot} + \frac{1}{2}k_{\mathrm{t}}\sum_{m=1}^{n-1}\mathrm{R}_{n-m}^{\cdot}\mathrm{R}_m^{\cdot} \qquad (51)$$

$$(1-\delta_{n,1}) \qquad n = 1,\ldots\infty$$

In the above equations, $\delta_{n,1}$ is the Kronecker delta, Y_0^{γ} ($\gamma = \cdot$, $\cdot$A, $\cdot$B, $\cdot\cdot$) are the zero order moments of macroradicals, M_0^{λ} (λ = A, B, AB, AA, BB) are the zero order moments of temporarily inactive polymers, and M_0 is the zero order moment of permanent polymer. These moments are a particular case of the general a^{th} order moment, $a = 0, 1, 2\ldots$, defined as shown in Eq. (52)

$$\mathrm{Y}_a^{\gamma} = \sum_{n=1}^{\infty} n^a \mathrm{R}_n^{\gamma} \qquad (52)$$

$$M_a^{\lambda} = \sum_{n=1}^{\infty} n^a \mathrm{P}_n^{\lambda}$$

The model assumes that the thermal stability of the peroxide in the macromolecule chains is independent of the chain length and that the termination by combination rate constants for all the macroradical species are identical.

The rate of change of the reaction mixture volume (V) is described by Eq. (53).

$$\frac{1}{V}\frac{\mathrm{d}V}{\mathrm{d}t} = -\frac{\epsilon}{M_{t=0}+\epsilon M}\frac{\mathrm{d}M}{\mathrm{d}t} \qquad (53)$$

where ϵ is the volume contraction factor and $M_{t=0}$ is the initial monomer concentration. The gel effect correlation suggested by Hui and Hamielec [10] for bulk styrene polymerization is used to account for the diffusion-controlled termination reactions at high monomer conversion. This correlation is shown in Table 1. The model considers that there is a single initiation efficiency for all peroxide groups, which is independent of conversion [1,9]. Kim [9] calculated optimal values of the efficiency factor by fitting data corresponding to $I_0 = 0.0042$, 0.0084 and 0.0126 mol/l, and found that the efficiency decreased linearly with initial peroxide concentration. Eq. (54) was used to calculate efficiencies in the model. It results from the linear regression of the efficiency values obtained at the three above mentioned initial initiator concentrations.

$$f = 0.6807 - 18.2I_0 \qquad (54)$$

2.1. pgf Balances

In order to model the MWD in this process we use the pgf technique [7,8]. pgf transformation is applied to the infinite set of mass balance equations of the macromolecular species, leading to a finite set of equations, where the dependent variable is the pgf transform of the MWD. The pgf calculated by solving the transformed equations, are then inverted to recover the MWD. Detailed description of the inversion methods that are used here can be found elsewhere [8,11,12].

pgf are defined for each macromolecule as shown in Eq. (55).

$$\varphi_a^{\gamma}(z) = \sum_{n=1}^{\infty} z^n \frac{n^a \mathrm{R}_n^{\gamma}}{\mathrm{Y}_a^{\gamma}} \qquad \gamma = \cdot, \cdot\mathrm{A}, \cdot\mathrm{B}, \cdot\cdot$$

$$\phi_a^{\lambda}(z) = \sum_{n=1}^{\infty} z^n \frac{n^a \mathrm{P}_n^{\lambda}}{M_a^{\lambda}} \qquad \lambda = A, B, AB, AA, BB, \qquad (55)$$

permanent polymer (no superscript) where $a = 0, 1, 2$.

It is also possible to define the pgf of the overall macromolecular species MWD [8], as shown in Eq. (56).

$$\overline{\phi}_a(z) = \frac{\sum_{\gamma}\mathrm{Y}_a^{\gamma}\varphi_a^{\gamma}(z) + \sum_{\lambda}M_a^{\lambda}\phi_a^{\lambda}(z)}{\sum_{\gamma}\mathrm{Y}_a^{\gamma} + \sum_{\lambda}M_a^{\lambda}} \qquad (56)$$

We have defined three types of pgf, identified by subscript $a = 0, 1, 2$ in the above equations, which represent the pgf transforms of the MWD expressed as number fraction vs. molecular weight (number distribution), weight fraction vs. molecular weight (weight distribution) or the product of weight fraction and molecular weight vs. molecular weight (chromatographic distribution). Inversion of each type of pgf allows the recovery of the three kinds of distribution independently, attenuating in this way numerical noise propagation [11].

The mass balances corresponding to macromolecules (Eqs. (42–51)) can be transformed into the pgf domain in a simple way by means of the pgf Transform Table we have previously developed [7,8], obtaining Eqs. (57–66).

Table 1
Kinetic parameters and initial conditions [9]

Kinetic constants	
k_{d_A}	$1.04 \times 10^{15} \exp(-33500/RT)\ s^{-1}$
k_{d_B}	$8.06 \times 10^{13} \exp(-29800/RT)\ s^{-1}$
k_{dm}	$2.190 \times 10^{5} \exp(-27440/RT)\ s^{-1}$
k_p	$1.051 \times 10^{7} \exp(-7060/RT)$ $1\ mol^{-1}\ s^{-1}$
k_{t0}	$1.260 \times 10^{9} \exp(-1680/RT)\ s^{-1}$
$k_i \approx k_p$	
k_{fm}	$7.807 \times 10^{6} \exp(-12940/RT)\ s^{-1}$
Gel effect	
$g \equiv k_t/k_{t0} = \exp[-2(Bx + Cx^2 + Dx^3)]$	
B	$2.57 - 5.05 \times 10^{-3}\ T$
C	$9.56 - 1.76 \times 10^{-2}\ T$
D	$-3.03 + 7.85 \times 10^{-3}\ T$
Initial conditions	
$M_{t=0}$	8.728 mol/l
$M^{\lambda}_{a,t=0} = Y^{\gamma}_{a,t=0} = \phi^{\lambda}_{a}(z)_{t=0} = \varphi^{\gamma}_{a}(z)_{t=0}$	$0 \forall a,\ a = 0, 1, 2$
Other parameters	
ϵ	-0.147

[R], cal/mol K [T], K; x, monomer conversion.

pgf of macroradicals

$$\frac{1}{V}\frac{\mathrm{d}((Y^{\cdot}_{a}\varphi^{\cdot}_{a}(z))V)}{\mathrm{d}t} = 2k_{dm}M^3 z + k_i R^{\cdot} M z + k_{d_A}(M^{A}_{a}\phi^{A}_{a}(z)) + k_{d_B}(M^{B}_{a}\phi^{B}_{a}(z)) + k_p M z \sum_{j=0}^{a}\binom{a}{j}(Y^{\cdot}_{j}\varphi^{\cdot}_{j}(z)) - k_p M(Y^{\cdot}_{a}\varphi^{\cdot}_{a}(z)) + k_{fm}M(Y^{\cdot}_{0} + Y^{\cdot A}_{0} + Y^{\cdot B}_{0} + 2Y^{\cdot\cdot}_{0})z + k_{fm}M(2(Y^{\cdot\cdot}_{a}\varphi^{\cdot\cdot}_{a}(z)) - (Y^{\cdot}_{a}\varphi^{\cdot}_{a}(z))) - k_t(Y^{\cdot}_{a}\varphi^{\cdot}_{a}(z))(Y^{\cdot}_{0} + Y^{\cdot A}_{0} + Y^{\cdot B}_{0} + 2Y^{\cdot\cdot}_{0}) + 2k_t\sum_{j=0}^{a}\binom{a}{j}(Y^{\cdot}_{a-j}\varphi^{\cdot}_{a-j}(z))(Y^{\cdot\cdot}_{j}\varphi^{\cdot\cdot}_{j}(z)) \quad a = 0, 1, 2 \tag{57}$$

$$\frac{1}{V}\frac{\mathrm{d}((Y^{\cdot A}_{a}\varphi^{\cdot A}_{a}(z))V)}{\mathrm{d}t} = k_i R^{\cdot A} M z - k_{d_A}(Y^{\cdot A}_{a}\varphi^{\cdot A}_{a}(z)) + k_{d_B}(M^{AB}_{a}\phi^{AB}_{a}(z)) + 2k_{d_A}(M^{AA}_{a}\phi^{AA}_{a}(z)) + k_p M z\sum_{j=0}^{a}\binom{a}{j}(Y^{\cdot A}_{j}\varphi^{\cdot A}_{j}(z)) - k_p M(Y^{\cdot A}_{a}\varphi^{\cdot A}_{a}(z)) - k_{fm}M(Y^{\cdot A}_{a}\varphi^{\cdot A}_{a}(z)) - k_t(Y^{\cdot A}_{a}\varphi^{\cdot A}_{a}(z))(Y^{\cdot}_{0} + Y^{\cdot A}_{0} + Y^{\cdot B}_{0} + 2Y^{\cdot\cdot}_{0}) + 2k_t\sum_{j=0}^{a}\binom{a}{j}(Y^{\cdot A}_{a-j}\varphi^{\cdot A}_{a-j}(z))(Y^{\cdot\cdot}_{j}\varphi^{\cdot\cdot}_{j}(z)) \quad a = 0, 1, 2 \tag{58}$$

$$\frac{1}{V}\frac{\mathrm{d}((Y^{\cdot B}_{a}\varphi^{\cdot B}_{a}(z))V)}{\mathrm{d}t} = k_i R^{\cdot B} M z - k_{d_B}(Y^{\cdot B}_{a}\varphi^{\cdot B}_{a}(z)) + k_{d_A}(M^{AB}_{a}\phi^{AB}_{a}(z)) + 2k_{d_B}(M^{BB}_{a}\phi^{BB}_{a}(z)) + k_p M z\sum_{j=0}^{a}\binom{a}{j}(Y^{\cdot B}_{j}\varphi^{\cdot B}_{j}(z)) - k_p M(Y^{\cdot B}_{a}\varphi^{\cdot B}_{a}(z)) - k_{fm}M(Y^{\cdot B}_{a}\varphi^{\cdot B}_{a}(z)) - k_t(Y^{\cdot B}_{a}\varphi^{\cdot B}_{a}(z))(Y^{\cdot}_{0} + Y^{\cdot A}_{0} + Y^{\cdot B}_{0} + 2Y^{\cdot\cdot}_{0}) + 2k_t\sum_{j=0}^{a}\binom{a}{j}(Y^{\cdot B}_{a-j}\varphi^{\cdot B}_{a-j}(z))(Y^{\cdot\cdot}_{j}\varphi^{\cdot\cdot}_{j}(z)) \quad a = 0, 1, 2 \tag{59}$$

$$\frac{1}{V}\frac{\mathrm{d}((Y^{\cdot\cdot}_{a}\varphi^{\cdot\cdot}_{a}(z))V)}{\mathrm{d}t} = 2k_i R^{\cdot\cdot} M z + k_{d_A}(Y^{\cdot A}_{a}\varphi^{\cdot A}_{a}(z)) + k_{d_B}(Y^{\cdot B}_{a}\varphi^{\cdot B}_{a}(z)) + 2k_p M z\sum_{j=0}^{a}\binom{a}{j}(Y^{\cdot\cdot}_{j}\varphi^{\cdot\cdot}_{j}(z)) - 2k_p M(Y^{\cdot\cdot}_{a}\varphi^{\cdot\cdot}_{a}(z)) - 2k_{fm}M(Y^{\cdot\cdot}_{a}\varphi^{\cdot\cdot}_{a}(z)) - 2k_t(Y^{\cdot\cdot}_{a}\varphi^{\cdot\cdot}_{a}(z))(Y^{\cdot}_{0} + Y^{\cdot A}_{0} + Y^{\cdot B}_{0} + 2Y^{\cdot\cdot}_{0}) + 2k_t\sum_{j=0}^{a}\binom{a}{j}(Y^{\cdot\cdot}_{a-j}\varphi^{\cdot\cdot}_{a-j}(z))(Y^{\cdot\cdot}_{j}\varphi^{\cdot\cdot}_{j}(z)) \quad a = 0, 1, 2 \tag{60}$$

pgf of temporary polymers

$$\frac{1}{V}\frac{\mathrm{d}((M_a^{\mathrm{A}}\phi_a^{\mathrm{A}}(z))V)}{\mathrm{d}t} = -k_{\mathrm{d_A}}(M_a^{\mathrm{A}}\phi_a^{\mathrm{A}}(z)) + k_{\mathrm{fm}}M(\mathrm{Y}_a^{\cdot\mathrm{A}}\varphi_a^{\cdot\mathrm{A}}(z)) + k_{\mathrm{t}}\sum_{j=0}^{a}\binom{a}{j}(\mathrm{Y}_{a-j}^{\cdot}\varphi_{a-j}^{\cdot}(z))(\mathrm{Y}_j^{\cdot\mathrm{A}}\varphi_j^{\cdot\mathrm{A}}(z)) \quad a=0,1,2 \tag{61}$$

$$\frac{1}{V}\frac{\mathrm{d}((M_a^{\mathrm{B}}\phi_a^{\mathrm{B}}(z))V)}{\mathrm{d}t} = -k_{\mathrm{d_B}}(M_a^{\mathrm{B}}\phi_a^{\mathrm{B}}(z)) + k_{\mathrm{fm}}M(\mathrm{Y}_a^{\cdot\mathrm{B}}\varphi_a^{\cdot\mathrm{B}}(z)) + k_{\mathrm{t}}\sum_{j=0}^{a}\binom{a}{j}(\mathrm{Y}_{a-j}^{\cdot}\varphi_{a-j}^{\cdot}(z))(\mathrm{Y}_j^{\cdot\mathrm{B}}\varphi_j^{\cdot\mathrm{B}}(z)) \quad a=0,1,2 \tag{62}$$

$$\frac{1}{V}\frac{\mathrm{d}((M_a^{\mathrm{AB}}\phi_a^{\mathrm{AB}}(z))V)}{\mathrm{d}t} = -(k_{\mathrm{d_A}}+k_{\mathrm{d_B}})(M_a^{\mathrm{AB}}\phi_a^{\mathrm{AB}}(z)) + k_{\mathrm{t}}\sum_{j=0}^{a}\binom{a}{j}(\mathrm{Y}_{a-j}^{\cdot\mathrm{A}}\varphi_{a-j}^{\cdot\mathrm{A}}(z))(\mathrm{Y}_a^{\cdot\mathrm{B}}\varphi_a^{\cdot\mathrm{B}}(z)) \quad a=0,1,2 \tag{63}$$

$$\frac{1}{V}\frac{\mathrm{d}((M_a^{\mathrm{AA}}\phi_a^{\mathrm{AA}}(z))V)}{\mathrm{d}t} = -2k_{\mathrm{d_A}}(M_a^{\mathrm{AA}}\phi_a^{\mathrm{AA}}(z)) + \frac{1}{2}k_{\mathrm{t}}\sum_{j=0}^{a}\binom{a}{j}(\mathrm{Y}_{a-j}^{\cdot\mathrm{A}}\varphi_{a-j}^{\cdot\mathrm{A}}(z))(\mathrm{Y}_j^{\cdot\mathrm{A}}\varphi_j^{\cdot\mathrm{A}}(z)) \quad a=0,1,2 \tag{64}$$

$$\frac{1}{V}\frac{\mathrm{d}((M_a^{\mathrm{BB}}\phi_a^{\mathrm{BB}}(z))V)}{\mathrm{d}t} = -2k_{\mathrm{d_B}}(M_a^{\mathrm{BB}}\phi_a^{\mathrm{BB}}(z)) + \frac{1}{2}k_{\mathrm{t}}\sum_{j=0}^{a}\binom{a}{j}(\mathrm{Y}_{a-j}^{\cdot\mathrm{B}}\varphi_{a-j}^{\cdot\mathrm{B}}(z))(\mathrm{Y}_j^{\cdot\mathrm{B}}\varphi_j^{\cdot\mathrm{B}}(z)) \quad a=0,1,2 \tag{65}$$

pgf of the permanent polymer

$$\frac{1}{V}\frac{\mathrm{d}((M_a\phi_a(z))V)}{\mathrm{d}t} = k_{\mathrm{fm}}M(\mathrm{Y}_a^{\cdot}\varphi_a^{\cdot}(z)) + \frac{1}{2}k_{\mathrm{t}}\sum_{j=0}^{a}\binom{a}{j}(\mathrm{Y}_{a-j}^{\cdot}\varphi_{a-j}^{\cdot}(z))(\mathrm{Y}_j^{\cdot}\varphi_j^{\cdot}(z)) \quad a=0,1,2 \tag{66}$$

These equations must be solved for different values of the dummy variable z as required by the inversion methods. In previous works [8,11,12] we have studied eight numerical inversion methods appropriate for the inversion of pgf of molecular weight distributions. Here we used Papoulis, Stehfest and IFG inversion methods [8,11,12]. The use of more than one inversion method helps to improve the reliability of the results [13].

Moments of macroradicals and polymers are required as data for the pgf balances. Hence, moment balances must be set up and solved together with the pgf balances. Details on the application of the well known moment technique may be found elsewhere [14]. Eqs. (67–76) present the moment balances for the different macromolecules.

a^{th} moments of macroradicals

$$\frac{1}{V}\frac{\mathrm{d}(\mathrm{Y}_a^{\cdot}V)}{\mathrm{d}t} = 2k_{\mathrm{dm}}M^3 + k_{\mathrm{i}}\mathrm{R}^{\cdot}M + k_{\mathrm{d_A}}M_a^{\mathrm{A}} + k_{\mathrm{d_B}}M_a^{\mathrm{B}} + k_{\mathrm{p}}M\sum_{j=0}^{a}\binom{a}{j}\mathrm{Y}_j^{\cdot} - k_{\mathrm{p}}M\mathrm{Y}_a^{\cdot} + k_{\mathrm{fm}}M(\mathrm{Y}_0^{\cdot}+\mathrm{Y}_0^{\cdot\mathrm{A}}+\mathrm{Y}_0^{\cdot\mathrm{B}}+2\mathrm{Y}_0^{\cdot\cdot}) + k_{\mathrm{fm}}M(2\mathrm{Y}_a^{\cdot\cdot}-\mathrm{Y}_a^{\cdot}) - k_{\mathrm{t}}\mathrm{Y}_a^{\cdot}(\mathrm{Y}_0^{\cdot}+\mathrm{Y}_0^{\cdot\mathrm{A}}+\mathrm{Y}_0^{\cdot\mathrm{B}}+2\mathrm{Y}_0^{\cdot\cdot}) + 2k_{\mathrm{t}}\sum_{j=0}^{a}\binom{a}{j}\mathrm{Y}_{a-j}^{\cdot}\mathrm{Y}_j^{\cdot\cdot} \quad a=0,1,2 \tag{67}$$

$$\frac{1}{V}\frac{\mathrm{d}(\mathrm{Y}_a^{\cdot\mathrm{A}}V)}{\mathrm{d}t} = k_{\mathrm{i}}R^{\cdot\mathrm{A}}M - k_{\mathrm{d_A}}\mathrm{Y}_a^{\cdot\mathrm{A}} + k_{\mathrm{d_B}}M_a^{\mathrm{AB}} + 2k_{\mathrm{d_A}}M_a^{\mathrm{AA}} + k_{\mathrm{p}}M\sum_{j=0}^{a}\binom{a}{j}\mathrm{Y}_j^{\cdot\mathrm{A}} - k_{\mathrm{p}}M\mathrm{Y}_a^{\cdot\mathrm{A}} - k_{\mathrm{fm}}M\mathrm{Y}_a^{\cdot\mathrm{A}} - k_{\mathrm{t}}\mathrm{Y}_a^{\cdot\mathrm{A}}(\mathrm{Y}_0^{\cdot}+\mathrm{Y}_0^{\cdot\mathrm{A}}+\mathrm{Y}_0^{\cdot\mathrm{B}}+2\mathrm{Y}_0^{\cdot\cdot}) + 2k_{\mathrm{t}}\sum_{j=0}^{a}\binom{a}{j}\mathrm{Y}_{a-j}^{\cdot\mathrm{A}}\mathrm{Y}_j^{\cdot\cdot} \quad a=0,1,2 \tag{68}$$

$$\frac{1}{V}\frac{\mathrm{d}(\mathrm{Y}_a^{\cdot\mathrm{B}}V)}{\mathrm{d}t} = k_{\mathrm{i}}\mathrm{R}^{\cdot\mathrm{B}}M - k_{\mathrm{d_B}}\mathrm{Y}_a^{\cdot\mathrm{B}} + k_{\mathrm{d_A}}M_a^{\mathrm{AB}} + 2k_{\mathrm{d_B}}M_a^{\mathrm{BB}} + k_{\mathrm{p}}M\sum_{j=0}^{a}\binom{a}{j}\mathrm{Y}_j^{\cdot\mathrm{B}} - k_{\mathrm{p}}M\mathrm{Y}_a^{\cdot\mathrm{B}} - k_{\mathrm{fm}}M\mathrm{Y}_a^{\cdot\mathrm{B}} - k_{\mathrm{t}}\mathrm{Y}_a^{\cdot\mathrm{B}}(\mathrm{Y}_0^{\cdot}+\mathrm{Y}_0^{\cdot\mathrm{A}}+\mathrm{Y}_0^{\cdot\mathrm{B}}+2\mathrm{Y}_0^{\cdot\cdot}) + 2k_{\mathrm{t}}\sum_{j=0}^{a}\binom{a}{j}\mathrm{Y}_{a-j}^{\cdot\mathrm{B}}\mathrm{Y}_j^{\cdot\cdot} \quad a=0,1,2 \tag{69}$$

$$\frac{1}{V}\frac{\mathrm{d}(\ddot{Y}_a V)}{\mathrm{d}t} = 2k_i \ddot{R} M + k_{d_A} \dot{Y}_a^A + k_{d_B} \dot{Y}_a^B + 2k_p M \sum_{j=0}^{a} \binom{a}{j} \ddot{Y}_j - 2k_p M \ddot{Y}_a - 2k_{fm} M \ddot{Y}_a - 2k_t \ddot{Y}_a (\dot{Y}_0 + \dot{Y}_0^A + \dot{Y}_0^B + 2\ddot{Y}_0) + 2k_t \sum_{j=0}^{a} \binom{a}{j} \ddot{Y}_{a-j} \ddot{Y}_j \qquad a = 0, 1, 2 \tag{70}$$

a^{th} moments of temporary polymers

$$\frac{1}{V}\frac{\mathrm{d}(M_a^A V)}{\mathrm{d}t} = -k_{d_A} M_a^A + k_{fm} M \dot{Y}_a^A + k_t \sum_{j=0}^{a} \binom{a}{j} \dot{Y}_{a-j} \dot{Y}_j^A \qquad a = 0, 1, 2 \tag{71}$$

$$\frac{1}{V}\frac{\mathrm{d}(M_a^B V)}{\mathrm{d}t} = -k_{d_B} M_a^B + k_{fm} M \dot{Y}_a^B + k_t \sum_{j=0}^{a} \binom{a}{j} \dot{Y}_{a-j} \dot{Y}_j^B \qquad a = 0, 1, 2 \tag{72}$$

$$\frac{1}{V}\frac{\mathrm{d}(M_a^{AB} V)}{\mathrm{d}t} = -(k_{d_A} + k_{d_B}) M_a^{AB} + k_t \sum_{j=0}^{a} \binom{a}{j} \dot{Y}_{a-j}^A \dot{Y}_a^B \qquad a = 0, 1, 2 \tag{73}$$

$$\frac{1}{V}\frac{\mathrm{d}(M_a^{AA} V)}{\mathrm{d}t} = -2k_{d_A} M_a^{AA} + \frac{1}{2} k_t \sum_{j=0}^{a} \binom{a}{j} \dot{Y}_{a-j}^A \dot{Y}_j^A \qquad a = 0, 1, 2 \tag{74}$$

$$\frac{1}{V}\frac{\mathrm{d}(M_a^{BB} V)}{\mathrm{d}t} = -2k_{d_B} M_a^{BB} + \frac{1}{2} k_t \sum_{j=0}^{a} \binom{a}{j} \dot{Y}_{a-j}^B Y_j^B \qquad a = 0, 1, 2 \tag{75}$$

a^{th} moment of permanent polymer

$$\frac{1}{V}\frac{\mathrm{d}(M_a V)}{\mathrm{d}t} = k_{fm} M \dot{Y}_a + \frac{1}{2} k_t \sum_{j=0}^{a} \binom{a}{j} \dot{Y}_{a-j} \dot{Y}_j \qquad a = 0, 1, 2 \tag{76}$$

These moments may be also used to calculate number (M_n) and weight (M_w) average molecular weights of the overall macromolecular species, as shown by Eqs. (77) and (78)

$$M_n = M_{mon} \frac{\sum Y_1^\gamma + \sum M_1^\lambda}{\sum Y_0^\gamma + \sum M_0^\lambda} \tag{77}$$

$$M_w = M_{mon} \frac{\sum Y_2^\gamma + \sum M_2^\lambda}{\sum Y_1^\gamma + \sum M_1^\lambda}$$

$$\gamma = \cdot, \cdot A, \cdot B, \cdot\cdot$$

$$\lambda = A, B, AB, AA, BB, \text{permanent polymer (no superscript)} \tag{78}$$

where M_{mon} is the monomer (styrene) molecular weight.

The system of differential equations to be solved consists of Eqs. (36–41), (53) and (57–76). Gear's method [15] for stiff systems was used to integrate these equations, with the kinetic parameters and initial conditions shown in Table 1. The resulting pgf of the individual macromolecular species together with the pgf of the global macromolecule mixture, calculated with Eq. (56), were fed to the inversion algorithms to recover the corresponding MWD. The MWD predicted with the three inversion methods used were coincident, something that indicates that none of the methods has numerical problems. As we lack experimental information on the complete MWD, the distributions predicted by the model are processed to calculate the average molecular weights M_n and M_w. The resulting average values are then compared with those calculated using Eqs. (77) and (78) and with experimental data reported by Kim [9].

Unlike other models of this process [1–5,9,16], we have not applied here the quasi-steady state assumption for radicals. This has allowed us to model the process near 100% monomer conversion, where the quasi-steady state hypothesis is no longer valid.

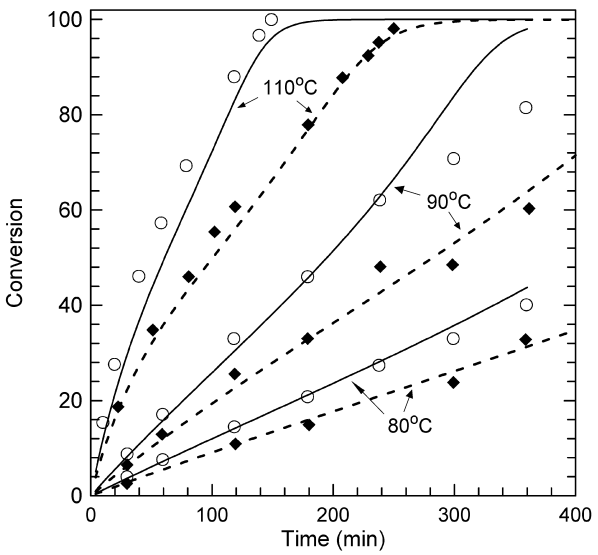

Fig. 1. Effect of polymerization temperature and initiator concentration on monomer conversion. Experimental data: (○) $I_0 = 0.0084$ mol/l, (◆) $I_0 = 0.0042$ mol/l; model predictions: (—) $I_0 = 0.0084$ mol/l ($f = 0.53$), (– – –) $I_0 = 0.0042$ mol/l ($f = 0.46$).

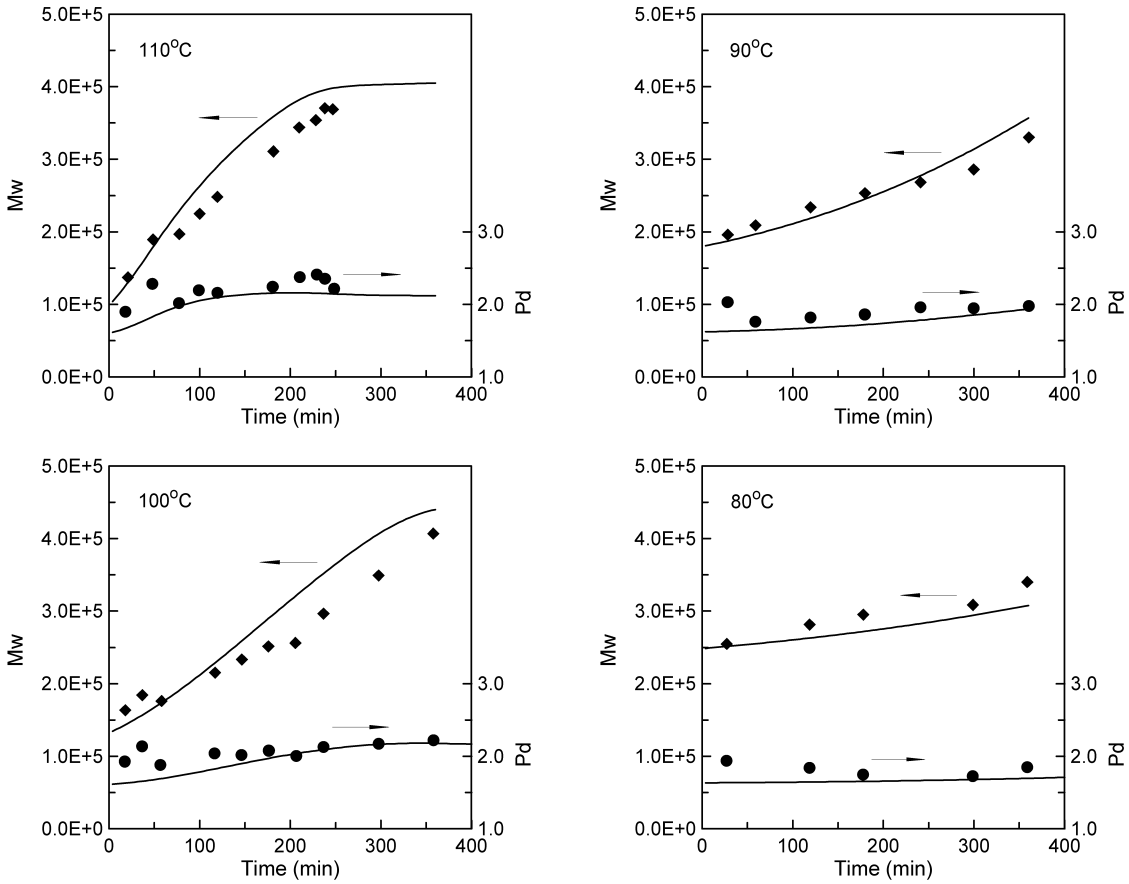

Fig. 2. Weight (M_w) average molecular weight and polydispersity (Pd) vs. reaction time, with $I_0 = 0.0042$ mol/l. (◆) experimental M_w, (●) experimental Pd, (—) model prediction with $f = 0.53$.

3. Results and discussion

Initiator concentration and temperature are the main operating parameters of this process. Fig. 1 shows the evolution of conversion and Fig. 2 of weight average molecular weight and polydispersity (Pd), with reaction time for different temperatures and peroxide concentrations. Model results are compared with experimental data reported in the work of Kim [9]. Two extra sets of conversion data at 100 °C were also compared, but omitted from Fig. 1 for clarity. Although figures similar to Figs. 1 and 2 of this work can be found in the work of Kim [9], we have included these graphics to show the good agreement of the model presented here with experimental values. Our model results and Kim's coincide for conversions and average molecular weights, which is logical as the same kinetic steps and kinetic parameters are used in both.

Fig. 1 shows that at any given initial initiator concentration reaction rate increases with temperature, and at any given temperature reaction rate increases with peroxide concentration. This is an expected result. Very good agreement with experimental information is achieved, except only at long reaction times for operating conditions of $T = 90$ °C and $I_0 = 0.0084$ mol/l.

Table 2
Comparison between average molecular weights calculated from the recovered MWD (M_n^d, M_w^d), calculated by the method of the moments (M_n^*, M_w^*), and experimental values (M_n^{exp}, M_w^{exp}) (9). The 'Relerr' column gives the percent relative error of the average molecular weights calculated from the MWD with respect to the experimental data

T (°C)	M_n^d	M_n^*	M_n^{exp}	Relerr	M_w^d	M_w^*	M_w^{exp}	Relerr
110	185,800	185,800	166,800	11.4	398,200	398,300	368,800	8.0
100	201,900	201,900	183,400	10.1	439,400	439,600	406,900	8.0
90	184,500	184,500	167,300	10.3	356,800	356,800	330,000	8.1
80	181,600	181,600	184,000	−1.3	307,700	307,700	340,100	−9.5

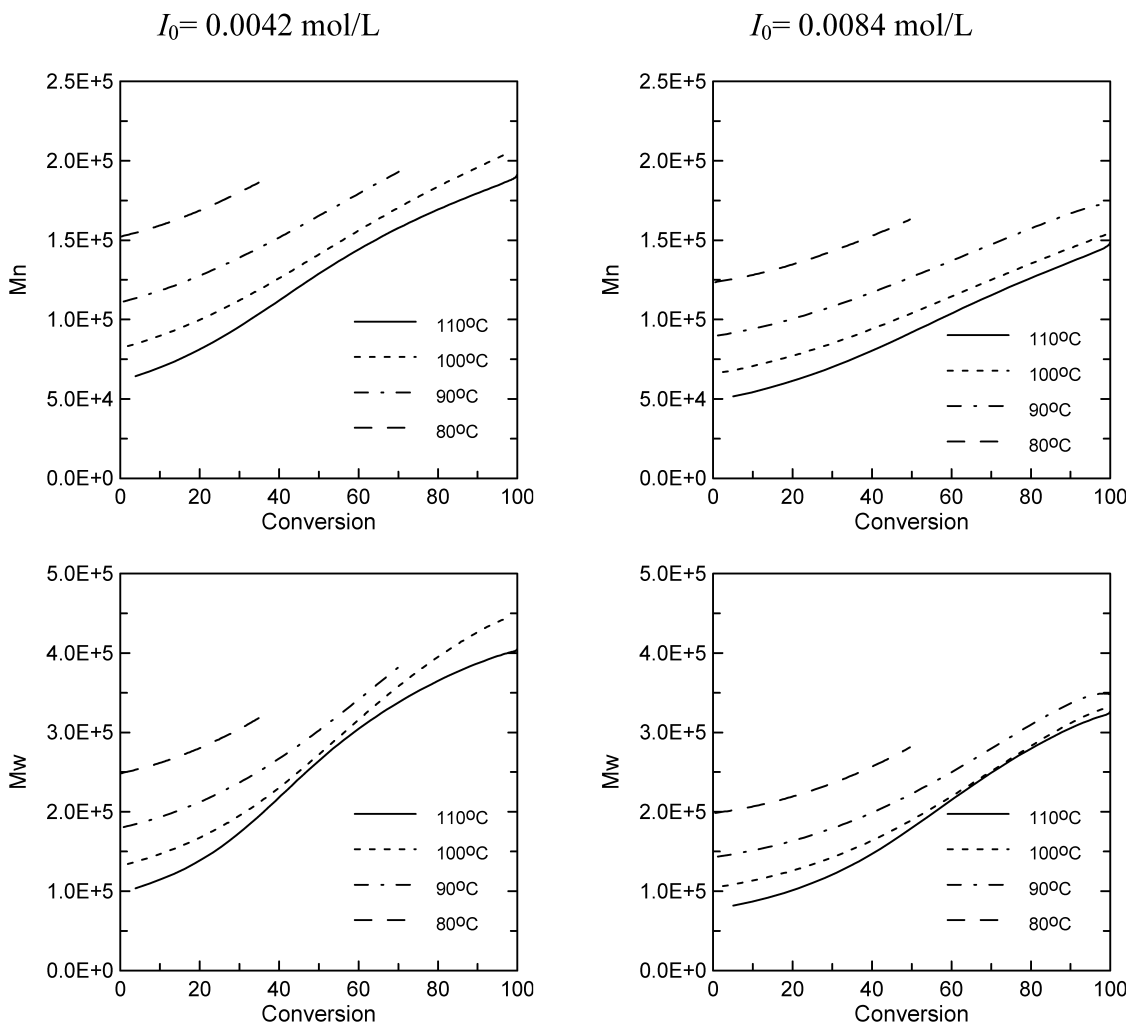

Fig. 3. Effect of polymerization temperature and initiator concentration on number (M_n) and weight (M_w) average molecular weights; reaction time, 360 min.

The model allows a satisfactory prediction of M_w and polydispersity (Pd), as Fig. 2 illustrates. The model results presented in this figure and also in Fig. 3 were obtained using Eqs. (77) and (78) (method of moments). Although the average molecular weights are overestimated at 100 and 110 °C, the overall agreement with experimental values is as good or better than what has been obtained with other reported models for this system [2,4,5,16]. In Fig. 3 we show the effect of temperature and initiator concentration on M_n and M_w. The results presented in this figure correspond to a reaction time of 360 min. As temperature increases, M_n and M_w become lower for equal monomer conversion. However, higher conversions can be achieved within the same reaction time due to the increase in polymerization rate, which may result in higher values of the average molecular weights, especially M_w. As expected, an increment in initiator concentration causes a reduction of the average molecular weights.

As we have already stated, the main purpose of this work is the prediction of the complete MWD in this process. Since we do not have experimental MWDs to compare with the theoretical predictions, we operate with them in order to calculate parameters that are available, such as M_n and M_w. In Table 2 we present a comparison between calculated values of M_n and M_w obtained from predicted MWDs and by the method of moments, in both cases rounded to the nearest hundred, together with experimental data. These experimental data correspond to the reaction conditions of the last experimental point in each of the four graphics in Fig. 2. As may be seen, the average molecular weights calculated from the MWD coincide with the ones calculated by the method of moments, and the relative error with respect to the experimental data is usually less than 10%. The same order of precision was obtained when predicting the remaining experimental points presented in Fig. 2.

Fig. 4 shows the MWD expressed in number, weight and chromatographic fraction basis, at different reaction times for temperatures of 80 and 100 °C. It can be seen that the MWDs shift to the right as the reaction proceeds, due to the generation of larger polymer molecules. At the same time the MWDs broaden, indicated by the lower height of the curves (all distributions have unit area). This behavior can

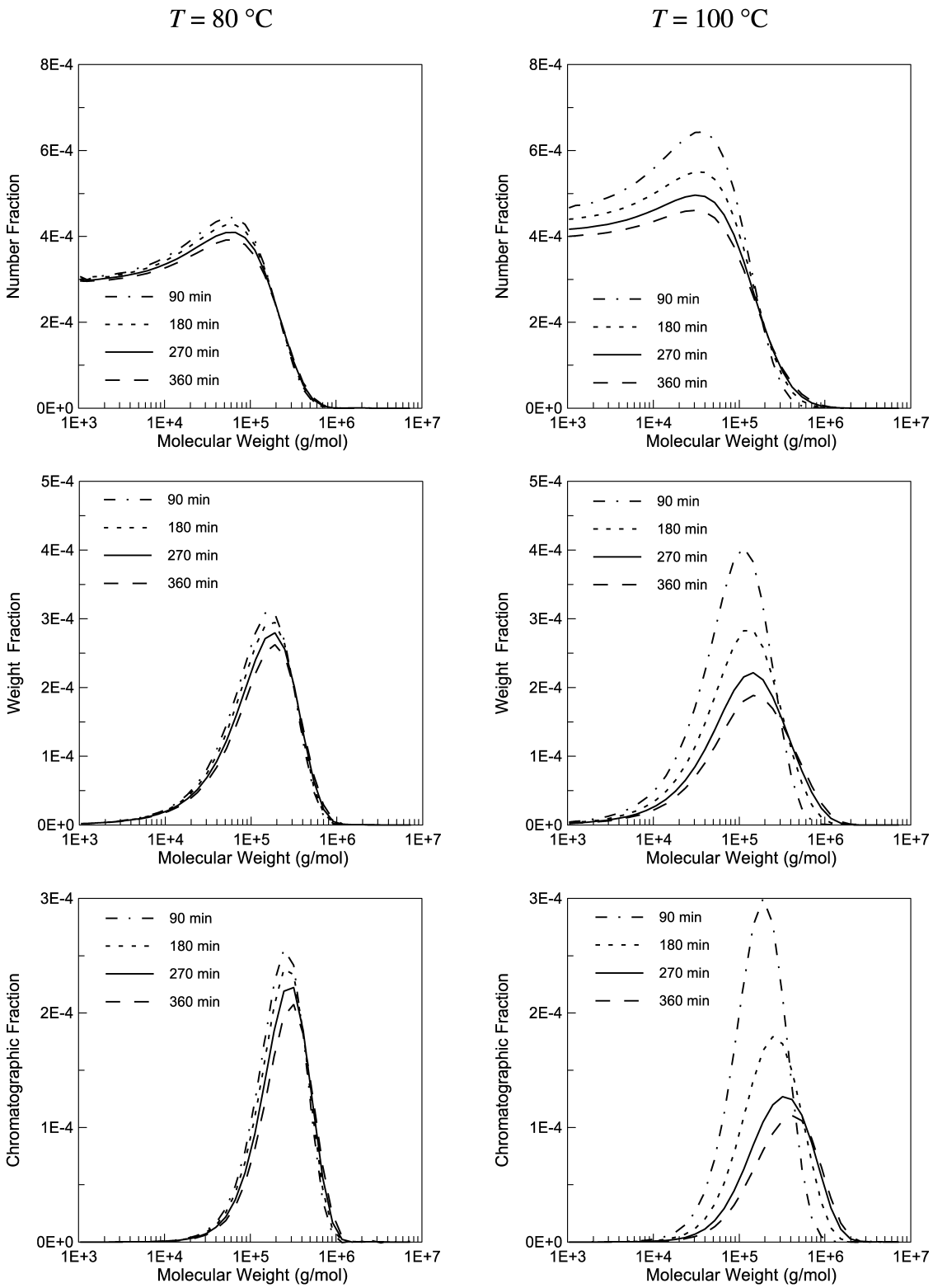

Fig. 4. Time evolution of the number, weight and chromatographic MWD for reaction temperatures of 80 and 100 °C; $I_0 = 0.0042$ mol/l.

be explained by the smaller rate of generation of initiation radicals as the reaction advances, due to the gradual consumption of initiator that results in lower initiator concentration. In addition to this, the use of bifunctional initiators originates a re-initiation-termination process that contributes to the appearance of even larger molecular weights. Distributions corresponding to a reaction temperature of 100 °C present a more important variation than those,

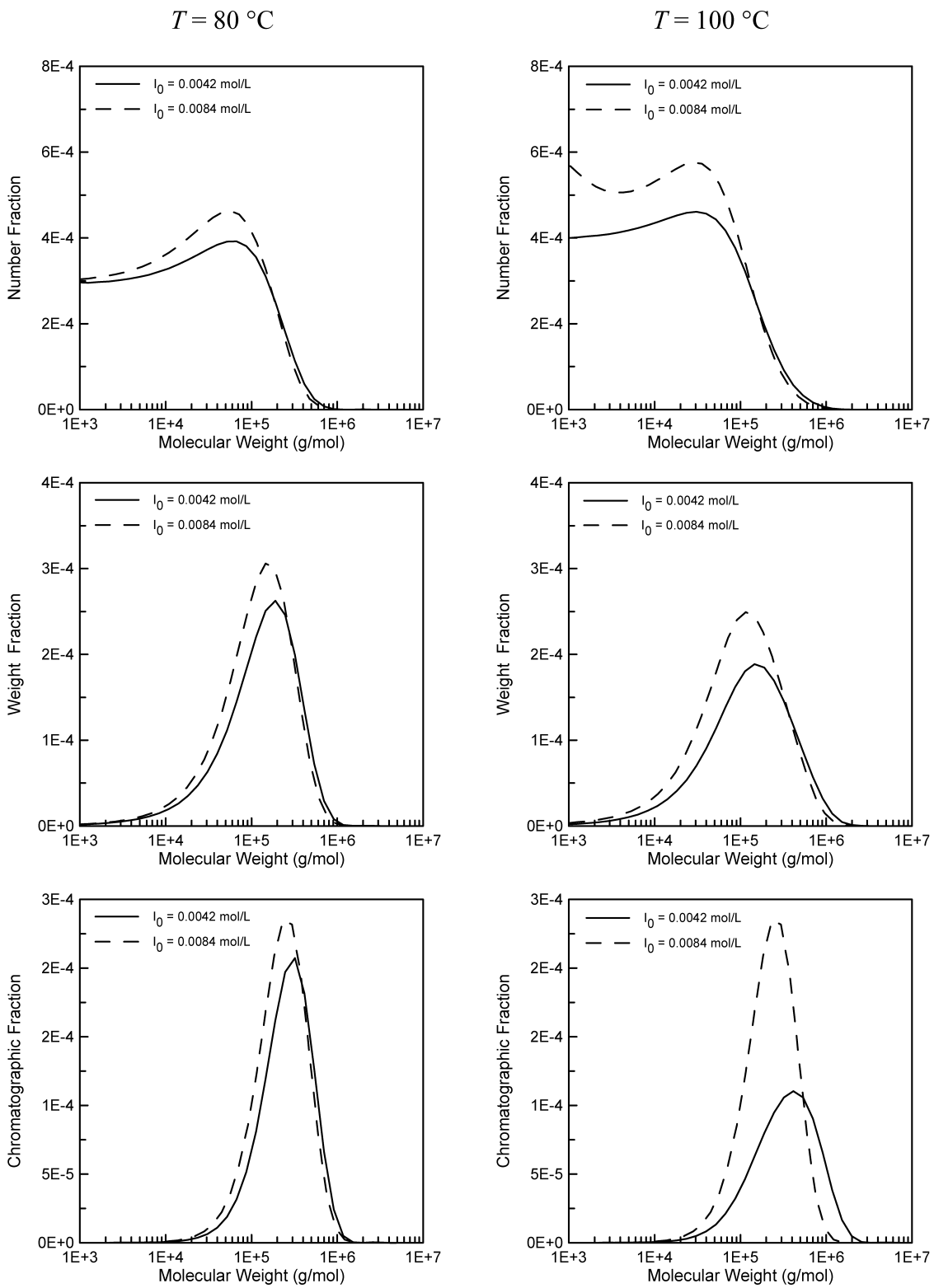

Fig. 5. Effect of initiator concentration on number, weight and chromatographic MWDs; reaction time, 360 min.

where the temperature is 80 °C because polymerization proceeds faster, so higher conversions are reached at equal reaction times.

Figs. 5 and 6 illustrate the effect of initiator concentration and temperature, respectively, on MWD. All MWDs shown in these figures correspond to a reaction time of 360 min. In Fig. 5, MWDs for $I_0 = 0.0042$ mol/l and $I_0 = 0.0084$ mol/l are compared at two different temperatures. Note that the lower I_0 results in distributions that are shifted to the right of the ones obtained with the higher I_0. This is reasonable since

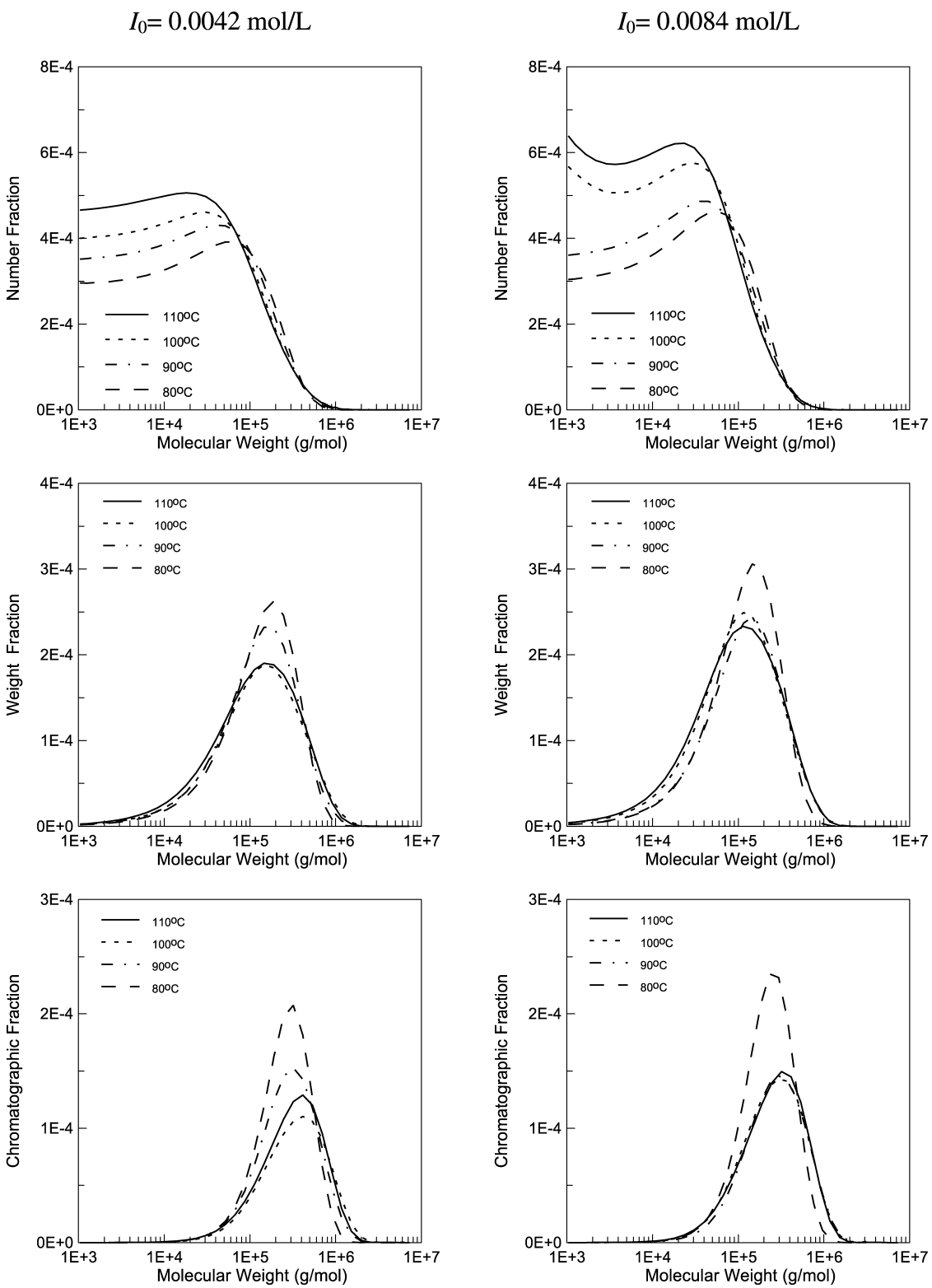

Fig. 6. Effect of polymerization temperature on number, weight and chromatographic MWDs; reaction time, 360 min.

at lower initiation concentrations fewer initiation radicals are available, resulting in higher molecular weights. In Fig. 6 MWDs parameterized by reaction temperature are shown for $I_0 = 0.0042$ mol/l and $I_0 = 0.0084$ mol/l. It is usual in polymerization reactions that, as temperature decreases, the decrease in the peroxide decomposition reaction rate is much more important than that of the propagation reaction rate. In consequence, there are fewer radicals to compete for the same amount of monomer, which should result in higher molecular weights at the lower temperatures. This is most

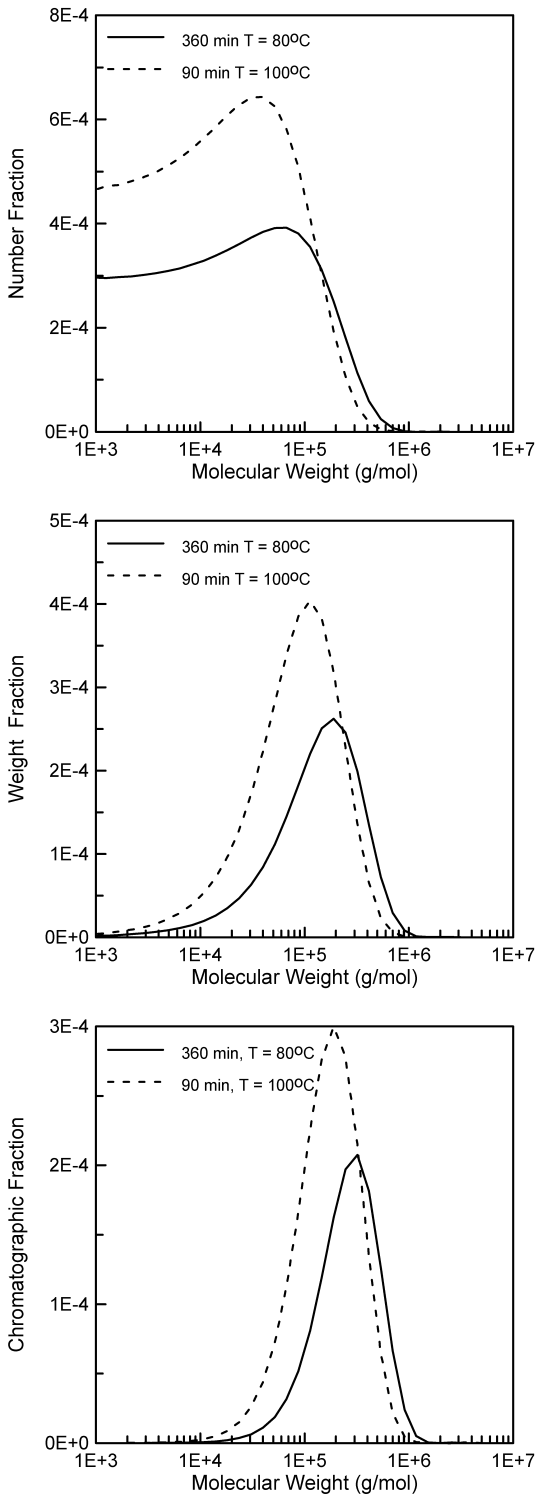

Fig. 7. Effect of temperature on number, weight and chromatographic MWDs; conversion, 32%; $I_0 = 0.0042$ mol/l.

easily observed in the number MWDs presented in this figure. Decreasing temperature makes molecular weight higher, but lower conversions are achieved as well. Thus, the high molecular weight tail is not as important as it might have been if higher conversions had been reached. This

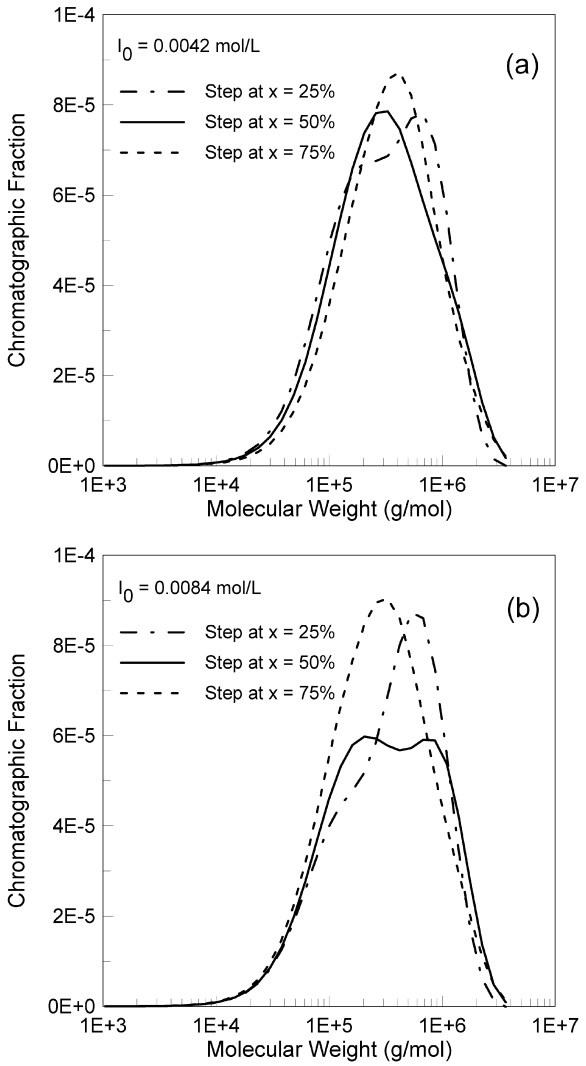

Fig. 8. Chromatographic MWD for polymerizations with a step temperature profile from 110 to 80 °C. Distributions are calculated for steps occurring when monomer conversion x has reached 25, 50 or 75%. Reaction time, 720 min.

explains why the lower molecular weight tails in the weight MWDs shown in Fig. 6 shift to the right as temperature rises (effect of higher molecular weights at lower temperatures), but the high molecular weight tails shift to the left (large molecules have not been produced owing to low conversion). For the same reason, the chromatographic MWDs, which are sensitive to the high molecular weight polymer, shift to the right at higher temperatures. At equal conversion, the whole MWD of the polymer synthesized at the lower temperature shifts to the right, as Fig. 7 exemplifies. In this figure we compare the distributions obtained at 80 °C and 360 min, and at 100 °C and 90 min. Under these conditions conversion is approximately 32% in both cases (see Fig. 1). It may be observed that the polymer produced at 80 °C presents higher molecular weight, which is consistent with the results presented in Fig. 3.

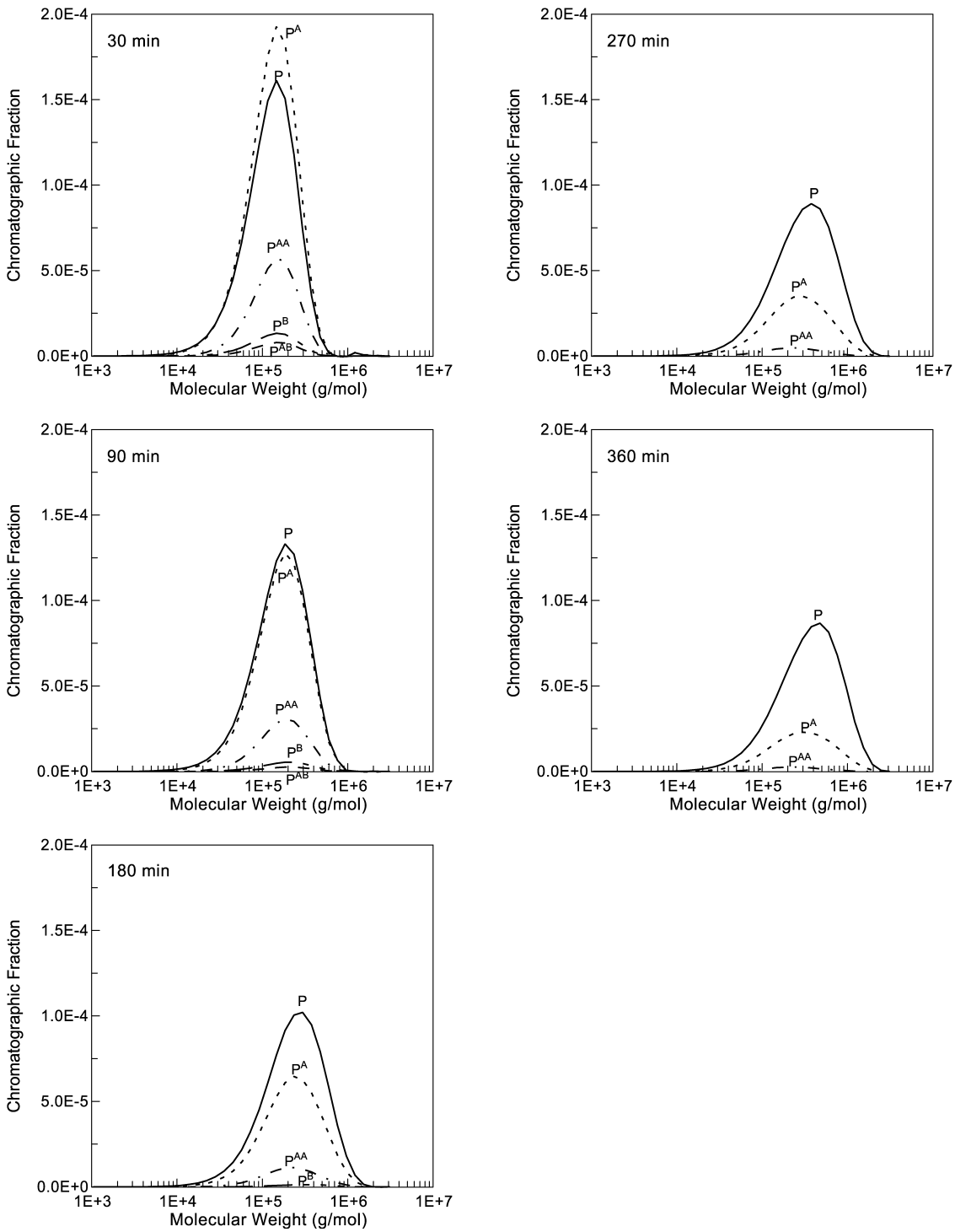

Fig. 9. Chromatographic MWDs of the permanent and temporary polymers at different reaction times; $I_0 = 0.0042$ mol/l and $T = 100$ °C.

One possible application of the model presented in this work is the design of molecular weight distributions to be obtained by tuning of operating conditions. When styrene is polymerized with bifunctional initiators, it is rather unlikely to obtain bimodal MWD under usual operating conditions [1]. Hence, as an example of how the model can be employed to achieve tailored polymers, we used it to find operating conditions that would lead to a bimodal MWD. We intended to accomplish bimodality by applying a step reduction in reaction temperature from 110 to 80 °C at a certain point along the reaction path. The sudden temperature decrease to 80 °C together with the fact that larger molecules are produced as the reaction goes on, would combine to produce a polymer of much higher molecular weight, and eventually result in a bimodal MWD. Fig. 8 shows the calculated chromatographic MWDs for

$I_0 = 0.0042$ mol/l (Fig. 8a) and $I_0 = 0.0084$ mol/l (Fig. 8b). Three different experiments were simulated for each case. They consisted in locating the step temperature reduction when monomer conversion x had reached 25, 50 and 75%, respectively. It can be seen in Fig. 8b that the MWD is unimodal when the step is at $x = 75\%$, but for a step at $x = 50\%$ a bimodal distribution is obtained. When the step occurs at $x = 25\%$, the higher molecular weight peak becomes more important so that the lower peak turns into a shoulder of the MWD. For $I_0 = 0.0042$ mol/l (Fig. 8a), we also obtained a MWD with a shoulder at the lower molecular weights when the step is at $x = 0.25\%$. However, unimodal MWDs result for $x = 50\%$ and $x = 75\%$ in this case. For the six polymerizations represented in Fig. 8, the reaction time was 720 min.

Another potential application of the model presented in this work is the design of block copolymer precursors, since knowledge of the MWD to be expected is of great value when bifunctional initiators are used in block copolymerization [6,17,18]. In particular, it is very important to know the distributions of the polymer species (resulting from the polymerization of the first co-monomer) with non-decomposed peroxide groups, which are used as macroinitiators for the polymerization of the second co-monomer. As an example of the capability of the model to predict the MWDs of the individual polymeric species, Fig. 9 shows the chromatographic distributions of the permanent and temporary polymers at different reaction times, corresponding to a polymerization carried out at $T = 100\,^{\circ}\mathrm{C}$ and $I_0 = 0.0042$ mol/l. The curves have been normalized so that they express the chromatographic fraction with respect to the global polymer, and thus their height is proportional to the amount of each species in the polymeric mixture. It may be seen that the permanent polymer predominates except at the early stages of the reaction, and that it presents the broader MWD. As expected, MWDs of the individual species shift to the right as the reaction proceeds. At the same time, the proportion of permanent polymer increases, due to the decomposition of the peroxide groups in the temporary polymers. Hence, short reaction times should be used if one is interested in a high amount of temporary polymer, e.g. to be used as macroinitiator in a copolymerization. Among the temporary polymers, those with a single peroxide-A group exhibit higher concentrations, followed by polymers with two peroxide-A groups. It should be remembered that the peroxide-A group has a smaller decomposition constant than the peroxide-B group.

4. Conclusions

A comprehensive mathematical model for styrene polymerization with asymmetric bifunctional initiators was developed, aiming at the prediction of not only productivity and average molecular properties as previous models did, but also the complete molecular weight distribution. Although the obtained distributions could not be compared with experimental ones, the average molecular weights calculated from them agree well both with experimental data and with calculations using the well-known moment technique.

The usefulness of the model was demonstrated evaluating the effect of different operating conditions on the MWD of the product. For example, the model allowed following MWD evolution in time, as well as its response to temperature and initiator concentration changes, giving a deeper insight into the process.

It was also possible to accommodate more complex situations such as polymerizations with an imposed temperature change during the course of a reaction. The ability of the model to predict temporary polymer MWD at different times was assessed, giving a tool to tailor block-copolymer precursors.

The model presented in this work has potential as a tool to tailor MWD of polymers obtained through the free radical mechanism using asymmetric initiators. Work is under way in which the model is employed in the simultaneous design and control of batch styrene polymerization processes posed as a single optimization problem.

Acknowledgements

The authors thank UNS,CONICET and ANPCyT for their financial support.

References

[1] Kim KJ, Choi KY. Chem Engng Sci 1989;44(2):297–312.
[2] Villalobos MA, Hamielec AE, Wood PE. J Appl Polym Sci 1991; 42(3):629–41.
[3] Benbachir M, Benjelloun D. Polymer 2001;42(18):7727–38.
[4] Cavin L, Rouge A, Meyer Th, Renken A. Polymer 2000;41(11): 3925–35.
[5] González IM, Meira GR, Oliva HM. J Appl Polym Sci 1996;59(6): 1015–26.
[6] O'Driscoll KF, Bevington JC. Eur Polym J 1985;21(12):1039–43.
[7] Asteasuain M, Sarmoria C, Brandolin A. Polymer 2002;43(8): 2513–27.
[8] Asteasuain M. Doctoral Thesis. Departamento de Ingeniería Química, Universidad Nacional del Sur, Argentina; 2003.
[9] Kim KJ. PhD Thesis. Department of Chemical Engineering, University of Maryland, USA; 1991.
[10] Hui AW, Hamielec AE. J Appl Polym Sci 1972;16:749–69.
[11] Brandolin A, Asteasuain M, Sarmoria C, López-Rodríguez A, Whiteley KS, Del Amo Fernández B. Polym Engng Sci 2001;41(7): 1156–70.
[12] Asteasuain M, Brandolin A, Sarmoria C. Polymer 2002;43(8): 2529–41.
[13] Davies B, Martin B. J Comp Phys 1979;33:1–32.
[14] Katz S, Saidel GM. AIChE J 1967;13(2):319–26.
[15] Gear CW. Numerical initial value problems in ordinary differential equations. NJ, USA: Englewood Cliffs; 1971.
[16] Yoon WJ, Choi KY. Polymer 1992;33(21):4582–91.
[17] Piirma I, Chou L-PH. J Appl Polym Sci 1979;24(9):2051–70.
[18] Gunesin BZ, Piirma I. J Appl Polym Sci 1981;26(9):3103–15.